ISSN 1063-7826, Semiconductors, 2017, Vol. 51, No. 11, pp. 1403–1408. © Pleiades Publishing, Ltd., 2017.
Original Russian Text © I.V. Erofeeva, M.V. Dorokhin, V.P. Lesnikov, Yu.M. Kuznetsov, A.V. Zdoroveyshchev, E.A. Pitirimova, 2017, published in Fizika i Tekhnika Poluprovodnikov, 2017, Vol. 51, No. 11, pp. 1456–1461.

XXI INTERNATIONAL SYMPOSIUM "NANOPHYSICS AND NANOELECTRONICS", NIZHNY NOVGOROD, MARCH 13–16, 2017

Thermoelectric Effects in Nanoscale Layers of Manganese Silicide

I. V. Erofeeva*, M. V. Dorokhin, V. P. Lesnikov, Yu. M. Kuznetsov, A. V. Zdoroveyshchev, and E. A. Pitirimova

Research Institute for Physics and Technology, Lobachevsky State University of Nizhny Novgorod, Nizhny Novgorod, 603950 Russia

**e-mail: irfeya@mail.ru*

Submitted April 27, 2017; accepted for publication May 12, 2017

Abstract—The values of the thermoelectric power, layer resistivity and thermal conductivity of a Mn_xSi_{1-x} nanoscale layer and Mn_xSi_{1-x}/Si superlattice on silicon depending on the growth temperature in the range $T = 300–600$ K are found experimentally. The contribution of the nanoscale film and substrate to the thermoelectric effect is discussed. The thermoelectric figure of merit of a single manganese-ssilicide layer, superlattice, and layer/substrate system is estimated. The largest figure of merit $ZT = 0.59 \pm 0.06$ is found for $Mn_{0.2}Si_{0.8}$ at $T = 600$ K.

DOI: 10.1134/S1063782617110112

1. INTRODUCTION

In recent decades, substantial progress has been attained in the field of the development and study of the properties of nanostructured thermoelectric materials. The specific features of the electronic structure of nanoscale objects can lead to a significant increase in coefficients that define the thermoelectric conversion efficiency. These specific features are due to the fact that the density of energy states near the Fermi level increases in nanoscale states and to the appearance of numerous interfaces, atomic defects, and other structural imperfections, which effectively scatter phonons but weakly affect the transport of charge carriers. Lattice thermal conductivity decreases due to phonon scattering at point defects and interfaces. This results in an increase in the figure of merit of the nanoscale thermoelectric material compared with a single-crystal sample.

For example, the thermoelectric figure of merit of nanostructured materials based on classic systems Bi_2Te_3, PbTe, SiGe, etc. turned out to be considerably higher compared with crystal analogs [1].

The selection of materials is based on requirements to the value of the efficiency of the thermoelectric converter and to the range of operating temperatures (each of the listed materials has the largest efficiency in a comparatively narrow temperature range). Higher manganese silicide is considered a promising material for the range of 400–600 K [2]. We can note studies on the development of nanostructures based on bulk manganese silicide [3–5]. We previously obtained polycrystalline thin films with an ultrafine granular crystal structure [6] and improved formation technologies of similar structures. In this study, we measured coefficients of the thermoelectric power, thermal conductivity, and resistivity of thin manganese-silicide layers and nanoscale Mn_xSi_{1-x}/Si superlattices grown on Si substrates and determined their thermoelectric figure of merit.

2. EXPERIMENTAL

The formation of thin Mn_xSi_{1-x} layers and Mn_xSi_{1-x}/Si nanostructures was performed using setup for pulsed laser deposition in vacuum by means of the sequential sputtering of Si (B-doped *p*-type Si with a resistivity of 12 Ω/sq.) and Mn targets. The composition of the layers was specified by the ratio of the sputtering times of Si and Mn targets. In this study, we formed layers with the ratio of sputtering times $t_{Mn}/t_{Si} = 1/4$, which approximately corresponds to the composition $Mn_{0.2}Si_{0.8}$. Homogeneous manganese-silicide layers were deposited on Si(100) substrates (B-doped *p*-type Si with a resistivity of 0.005 Ω/sq.) at a temperature of $T = 300$°C (sample *A*). This temperature mode is optimal for the formation of materials with superstructure ordering as was found in previous experiments [4, 6]. A multilayered structure, which consists of ten alternating nanoscale Mn_xSi_{1-x} and Si layers ($[Mn_xSi_{1-x}/Si]_{10}$—sample *B*) was formed under the same conditions on Si(100) substrates. The composition of manganese silicide in homogeneous layers and in the superlattice periods of the Mn_xSi_{1-x} coincides. The total layer thickness was estimated by the growth time being in both cases ~44 nm. A schematic of the structures is shown in Fig. 1a.

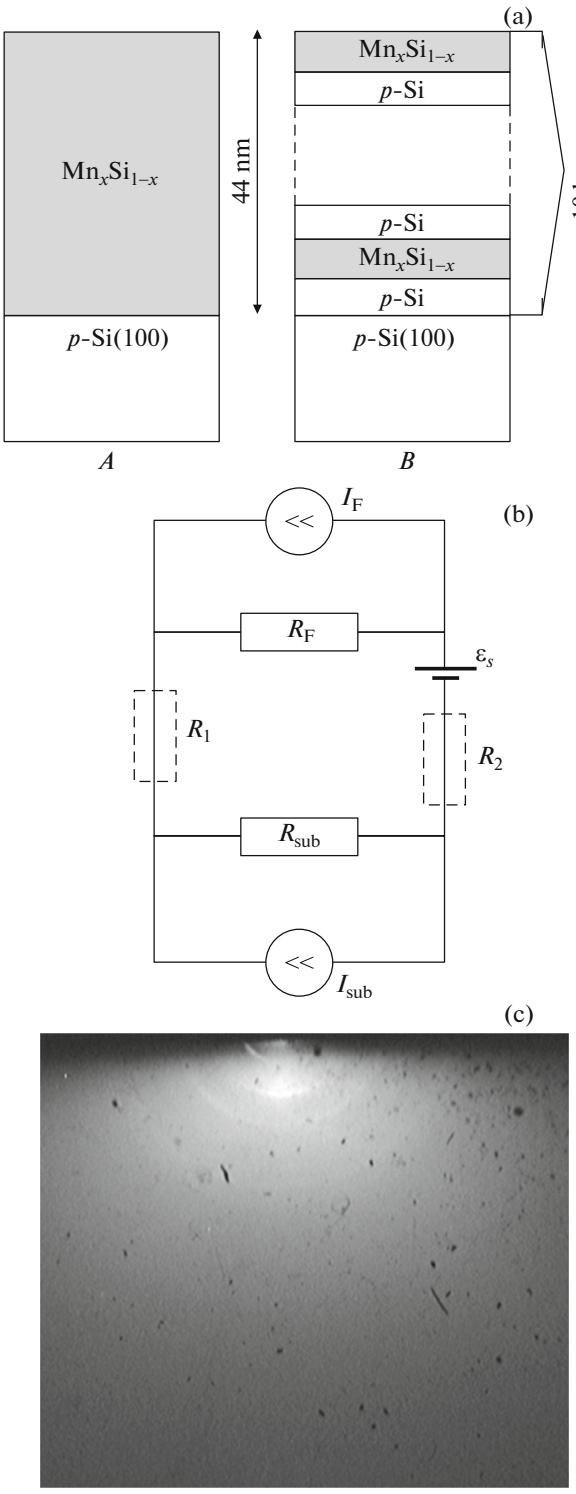

Fig. 1. (a) Schematics of the studied structures: *A* is the Mn_xSi_{1-x}/Si structure and *B* is the $[Mn_xSi_{1-x}/Si]_{10}$/Si superlattice; (b) equivalent electric circuit of the structure containing layers based on manganese silicide deposited onto the Si substrate. Directions of the currents of current sources and polarities of the source of thermoelectric power are denoted conditionally and can differ from the true ones; and (c) electron diffraction pattern of the surface of the Mn_xSi_{1-x} layer (*A*) deposited onto the Si(100) substrate.

Studies into the crystal structure of the formed manganese-silicide layers are carried out through the use of reflection electron diffractometry. Figure 1*c* shows the electron diffraction pattern of the surface of the manganese-silicide layer (sample *A*). Comparatively spread rings are observed in the electron diffraction pattern, which corresponds to the fine-grained polycrystalline structure. We note that the view of electron diffraction patterns for all studied structures is identical and corresponds to the fine-grained structure. The formation of layers with this type of crystalline structure is associated with selected deposition modes [4, 6]. It is considered that the formation of thermoelectric materials with a polycrystalline structure is preferential because phonon scattering at grain boundaries leads to a decrease in the phonon component of the thermal conductivity and, consequently, to an increase in the coefficient of the thermoelectric figure of merit [6].

To determine the Seebeck coefficient and resistivity, Au-based ohmic contacts were deposited onto the surface of structures. The thermoelectric power and resistivity were measured in a vacuum chamber at a residual pressure of 10^{-3} Torr in the temperature range 300–600 K. When measuring the thermoelectric power, the sample was located on a conducting graphite plate heated by the radiation of a halogen lamp and was electrically insulated from it by a thin mica layer. The temperature gradient between the sample edges was formed by means of increased heat removal from one edge (the cold end). The graphite plate temperature was set and maintained constant (±1 K). The temperature of the hot and cold sample ends was recorded using thermocouples. The temperature difference at the sample ends increases under experimental conditions with an increase in the heater temperature. The measurement circuit of the resistivity of the layers coincided with the that of the thermoelectric power, but heat removal at the sample ends was not different (i.e., the sample was maintained at a constant temperature in the range under study). Vacuum pumping to 10^{-3} Torr was performed to decrease heat removal from the heated sample regions by the air medium [7].

The thermal-conductivity coefficient was measured using the same vacuum system. To measure the thermal-conductivity coefficient, we used the frequency separation method (3w method). The essence of the method consists in measurement of the temperature gradient formed in the measured material due to current flow along a thin metallic conductor specially deposited onto the surface of this material [8–10]. The metal conductor ("a hot strip") serves simultaneously as the heating source and a temperature sensor (the variation in temperature is recorded by a variation in the strip resistance).

In our measurement circuit, a metallic strip was deposited onto a thin dielectric layer (10-nm Al_2O_3

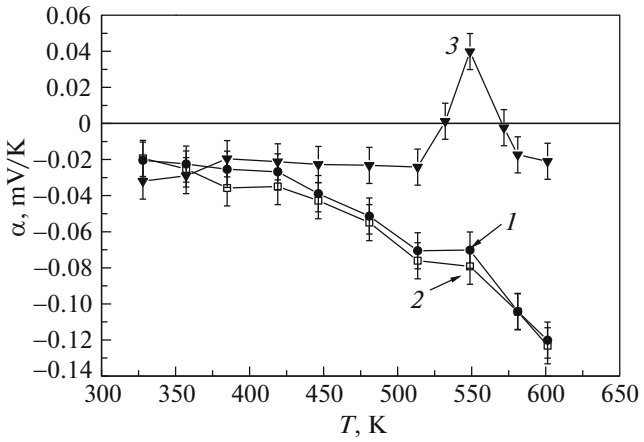

Fig. 2. Temperature dependence of the Seebeck coefficient: (*1*) single Mn_xSi_{1-x} layer (sample *A*), (*2*) superlattice (sample *B*), and (*3*) Si substrate with the resistivity of 0.005 Ω/sq.

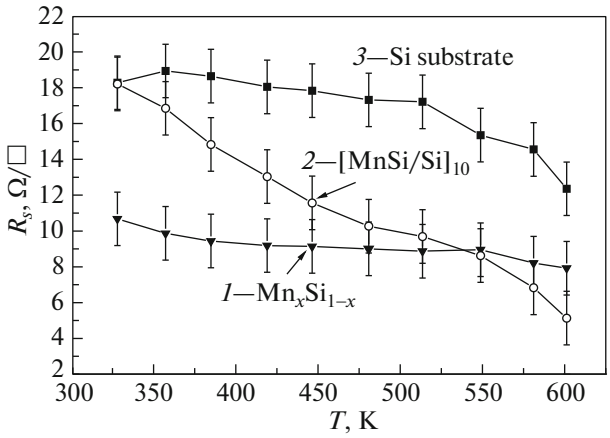

Fig. 3. Temperature dependence of the layer resistance: (*1*) single Mn_xSi_{1-x} layer (sample *A*), (*2*) superlattice (sample *B*), and (*3*) Si substrate.

layer) in order to avoid leakage of the electric current to the conducting semiconductor structure. To measure the thermal conductivity of thin manganese-silicide films and take into account the thermal conductivity of the Al_2O_3 layer, we used the improved measurement procedure of thin films proposed in [11–13]. The essence of the procedure consists in consideration of the film as a thermal resistor varying the maximal substrate temperature. The comparison of this result with the results of measuring the thermal-conductivity coefficient of a substrate makes it possible to calculate the target thermal-conductivity coefficient of the layer.

3. MEASUREMENT OF THE SEEBECK COEFFICIENT

Figure 2 shows the temperature dependences of the Seebeck coefficient for Mn_xSi_{1-x} layers (curve *1*) and $[Mn_xSi_{1-x}/Si]_{10}$ superlattices (curve *2*) formed on Si substrates. The temperature dependence of the thermoelectric power of the Si substrate is also presented on the plot (curve *3*). The Seebeck coefficient for the Si substrate is negative in the larger part of the temperature range, which corresponds to hole conductivity [14]. We note an abrupt peak at a temperature of ~540 K in the temperature dependence of the Seebeck coefficient. Herewith, the thermoelectric power changes sign to positive in a narrow temperature range near 540 K, which is apparently caused by the thermal activation of deep donor centers (the estimated value of the activation energy is 50 meV).

The value of both the thermoelectric power and the Seebeck coefficient is negative in the studied temperature range, which also corresponds to hole conductivity. The Seebeck coefficient steadily increases in absolute value in the range of 330–600 K (the coefficient sign <0 herewith). The largest value was −0.12 mV/K at 600 K. We note that the magnitude of the Seebeck coefficient in the temperature range of 300–400 K coincides within the experimental error with the value found for the Si substrate, which can evidence the influence of the substrate on the thermoelectric power in the given temperature range. The thermoelectric power of the studied structures at $T > 400$ K exceeds that for the Si substrate, which evidences the influence of the deposited layer on the observed Seebeck effect.

4. MEASUREMENT OF THE LAYER RESISTANCE

Temperature dependences of the resistance of structures are presented in Fig. 3. The resistance of the Si substrate slightly depends on temperature in the studied range and lies within the limits of 10–20 Ω/□ (curve *3*). Apparently, we have impurity conduction of the low-ohmic substrate over the entire temperature range, which is determined by the doping level (~10^{19} cm^{-3}). The temperature dependences of the resistance of the Mn_xSi_{1-x} layer and the $[Mn_xSi_{1-x}/Si]_{10}$ structure are presented in Fig. 3 (curves *1* and *2*, respectively). A weak dependence of the layer resistance on the measurement temperature in the selected range is found for the structure with a single manganese-silicide layer. On the contrary, the resistance for the structure with the $[Mn_xSi_{1-x}/Si]_{10}$ superlattice steadily decreases with increasing temperature, and the resistance of the structure with the $[Mn_xSi_{1-x}/Si]_{10}$ superlattice is close to the substrate resistance near room temperature.

5. RESULTS AND DISCUSSION

To take into account the influence of substrates on the Seebeck coefficient, we proposed the simplest model based on consideration of the equivalent electric circuit (Fig. 1*b*). The thermoelectric power of the film and a substrate are taken into account by current sources I_f and I_{sub}, respectively. Resistors R_f and R_{sub} take into account the resistances of the film and the substrate at the average temperature $(T_h - T_c)/2$, where T_h is the temperature of the "hot" sample end and T_c is the temperature of the "cold" sample end. The thermoelectric power of the substrate is

$$\varepsilon_{sub} = I_{sub}R_{sub}, \quad (1)$$

while the thermoelectric power of the film is

$$\varepsilon_f = I_f R_f. \quad (2)$$

Let us accept that the film resistance in the perpendicular direction (between the contact and the substrate) is much smaller than the resistance along the film (between the contact to the "hot" and "cold" sample ends). This assumption is justified if the contact formed on the structure surface is diffusive and simultaneously ensures an electrical connection both to the substrate and to the layer. The possible presence of a potential barrier between the manganese-silicide layer and the Si substrate is taken into account by means of introducing additional resistors R_1 and R_2. In the case of the formation of a potential barrier between the contacts to the "hot" and "cold" sample ends, an additional contact thermoelectric power can appear, which is taken into account by source ε_x in the equivalent circuit.

When considering the simplest case ($R_1 = R_2 = 0$, $\varepsilon_x = 0$), which corresponds to the Mn_xSi_{1-x}/Si low-barrier contact, we can show that the measured thermoelectric power associated with the substrate equals

$$\varepsilon'_{sub} = I_{sub}R_{sub}R_f/(R_{sub} + R_f), \quad (3)$$

which is smaller than the thermoelectric power of the substrate by quantity $(R_{sub} + R_f)/R_f$. The substrate contribution to the thermoelectric power is determined by the ratio of the substrate and film resistances. The contribution of the thermoelectric power of the film to the total measured magnitude of the thermoelectric power (ε'_f) similarly depends on the substrate resistance:

$$\varepsilon'_f = I_f R_f R_{sub}/(R_{sub} + R_f). \quad (4)$$

For a low-ohmic substrate, this contribution is minimal, while in the case $R_{sub} \gg R_f (R_{sub}/(R_{sub} + R_f) \approx 1)$, the contribution of the thermoelectric power of a film is maximal and equals ε_f.

The considered equivalent circuit allows us to analyze the results of studying the Mn_xSi_{1-x}/KDB-0.005 and $[Mn_xSi_{1-x}/Si]_{10}$/KDB-0.005 systems. The magnitude of the thermoelectric power of both a single manganese-silicide layer and superlattice in the temperature range of 300–400 K is close to the thermoelectric power of the substrate, while the layer resistance is comparable or higher than the substrate resistance. This fact evidences an insignificant contribution of the studied layers to the measured thermoelectric power (apparently, the main contribution in the range of 300–400 K is provided by the substrate). When increasing the measurement temperature above 400 K, the thermoelectric power of both structures abruptly increases and becomes higher than the thermoelectric power of the substrate. By virtue of the fact that the resistances of the layers and the substrate in the mentioned range are also comparable (while the superlattice resistance is somewhat lower than that of the substrate), we can assume that the layers under study introduce the main contribution to the Seebeck coefficient. Herewith, the contribution ε_{sub} of the substrate is reduced to a certain value in the total thermoelectric power due to inclusion of the parallel substrate resistance into the equivalent circuit. We also note the appearance of the local maximum at 550 K in the temperature dependences of the Seebeck coefficient found for both structures. The assumption that this maximum is associated with the contribution ε_{sub} of the substrate to the Seebeck coefficient (the thermoelectric power of the Si substrate is positive at the mentioned temperature) is quite justified.

6. ESTIMATION OF THE THERMOELECTRIC FIGURE OF MERIT

To estimate the efficiency of the thermoelectric conversion of the formed structures, we calculated the thermoelectric figure of merit coefficient. The term "thermoelectric figure of merit" is usually understood as a dimensionless coefficient, which is determined as

$$ZT = \alpha^2 \sigma T/\lambda, \quad (5)$$

where α is the Seebeck coefficient, which determines the voltage formed by an element at a specified temperature difference; σ is the electrical conductivity; T is the temperature; and λ is the thermal-conductivity coefficient.

To calculate the coefficient ZT of the studied layers, we calculated the magnitude α from the dependences presented in Fig. 2 applying formulas (3) and (4) in correspondence with the assumption of the equivalent circuit and the principle of superposition. Starting from (4), the true value of the Seebeck coefficient of the film can be written as

$$\alpha = \alpha_{mes}(R_{sub} + R_f)/R_{sub} - \alpha_{sub}(R_{sub} + R_f)/R_f, \quad (6)$$

where α_{sub} is the measured value of the Seebeck coefficient of the substrate and α_{mes} is the measured value

Table 1. Measured and published values of the thermal-conductivity coefficients of the manganese-silicide layers and $[Mn_xSi_{1-x}/Si]_{10}$ superlattices

Sample	T, K						
	300	350	400	450	500	550	600
$\lambda(A)$, W/(m K)	1.54 ± 0.25	1.27 ± 0.21	1.2 ± 0.21	1.15 ± 0.19	–	–	–
$\lambda(B)$, W/(m K)	1.77 ± 0.31	1.36 ± 0.22	1.26 ± 0.21	1.05 ± 0.19	–	–	–
According to published data [2, 15]	2.3	2.3	2.3	2.3	2.3	2.3	2.4

Table 2. Values of the coefficient of the thermoelectric figure of merit for studied structures

Sample no.	Layer type	ZT of the layer*	averaged ZT**
A	Mn_xSi_{1-x}	0.59 ± 0.06	$(0.92 \pm 0.1) \times 10^{-4}$
B	$[Mn_xSi_{1-x}/Si]_{10}$	0.37 ± 0.04	$(0.67 \pm 0.1) \times 10^{-4}$
Si	Substrate	10^{-6}	

*Maximal found values are presented as ZT. **When calculating the averaged ZT coefficient, averaged values of the thermal conductivity and resistance were used.

of the Seebeck coefficient for the film/substrate structures.

The electrical conductivity of the films was calculated from dependences presented in Fig. 3 by the formula for parallel resistors:

$$R_f = R_{sub}R_{mes}/(R_{mes} - R_{sub}), \quad (7)$$

where R_{mes} is the measured resistance of film/substrate structures.

The thermal-conductivity coefficient was measured in the temperature range 300–450 K. The results are shown in Table 1. Leakage currents from a metallic strip (heating sources and measurer) into measured semiconductor layers through a dielectric become substantial at a temperature above 450 K. This effect substantially increases the measurement error of λ. To find the estimate of λ for temperatures of 480–600 K, let us refer to published data [2, 15]. In cited publications, the measured values of the thermal-conductivity coefficient λ are presented for higher manganese silicide: in the temperature range of 300–600 K, λ ≈ 2 W/(m K) and is almost independent of the measurement temperature. In our study, we found close although smaller values of λ for the temperature range of 300–450 K, which can be associated with the fact that the structures under study are polycrystals, while the magnitude of λ for polycrystals is usually lower than for a single crystal. Admitting the invariability of the thermal-conductivity coefficient for the studied layers at 450 K < T < 600 K, let us accept as a rough estimation that λ equals 1 W/(m K) in the temperature range of 480–600 K.

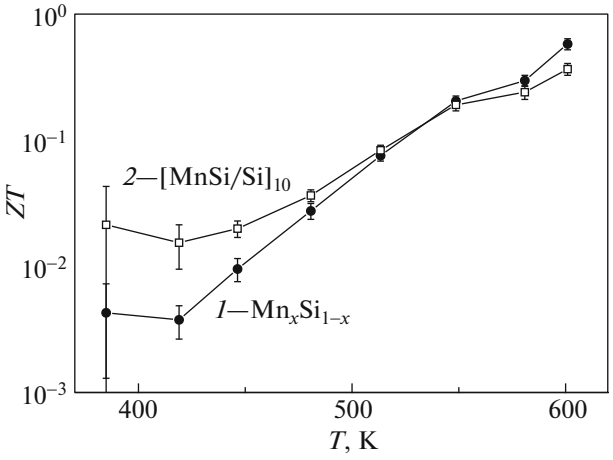

Fig. 4. Temperature dependence of the coefficient of the thermoelectric figure of merit (ZT) of structures *A* (curve *1*) and *B* (curve *2*).

Based on our calculations and presented considerations, we calculated the thermoelectric figure of merit according to formula (5). The results for layers Mn_xSi_{1-x}/Si and $[Mn_xSi_{1-x}/Si]_{10}/Si$ are presented in Fig. 4 and in Table 2. The results are acquired starting from an assumption of the isotropic character of the thermal conductivity (the thermal-conductivity coefficient in the direction perpendicular to the layer plane is close to the in-plane thermal-conductivity coefficient). A steady increase in ZT takes place for both types of structures with an increase in the measurement temperature to 600 K. According to known published data, the maximum of the figure of merit for the higher manganese silicide is observed near the temperature of 700 K being ~0.2 [2, 6, 15]. This fact allows us to assume that our value $ZT = 0.59 \pm 0.06$ is close to maximal. We also note that the measured values of ZT in the low-temperature region are inexact because of a considerable contribution of R_{sub} of the substrate. However, by virtue of a low Seebeck coefficient for

studied layers in the mentioned range, these values have no practical interest.

7. CONCLUSIONS

Thus, it is shown that the use of nanoscale layers based on manganese silicide with an ultrafine-grained polycrystalline structure makes it possible to acquire an increased thermoelectric figure of merit. We note that investigations did not reveal a substantial difference between the thermoelectric power and ZT for structures based on homogeneously doped Mn_xSi_{1-x} layers and $[Mn_xSi_{1-x}/Si]_{10}$ superlattices. We can assume that by virtue of the diffusion of manganese atoms and similar growth modes, the samples have similar crystal structures. The total decrease in the manganese concentration apparently does not lead to a substantial variation in the thermoelectric-power mechanisms in the structures.

We should also emphasize that the values of ZT presented in Fig. 4 are fundamental thermoelectric characteristics of Mn_xSi_{1-x} or $[Mn_xSi_{1-x}/Si]_{10}$ layers because they were found by calculation of the resistance of these layers and by estimation of their contribution to the thermoelectric power. From the practical viewpoint, in order to estimate ZT, we should consider the properties of the entire structure, i.e., the substrate with the layer deposited onto it. To estimate the coefficient of the thermoelectric figure of merit, we should consider the values of the thermoelectric power found directly for the studied structure and introduce the averaged value of the resistivity taking into account the substrate resistance and the averaged value of the thermal conductivity. Such an analysis was performed, and the data are presented in Table 2. It is seen that the thus calculated values are substantially underestimated relative to the values of ZT for the studied layers. It is evident that thermoelectric materials based on nanoscale layers do not make it possible to accumulate a sufficient amount of electric charge to create high-power supply sources (we speak about the total power rather than the specific power). At the same time, the thermoelectric figure of merit for the structure with a film is considerably larger than ZT found for the Si substrate. Therefore, we can conclude that the use of nanoscale films has practical potential.

ACKNOWLEDGMENTS

This study was supported by the Ministry of Education and Science of the Russian Federation (projects no. 8.1751.2017/PCh and 16.7443.2017/BCh), by the Russian Foundation for Basic Research, project nos. 15-02-07824_a and 16-07-01102_a, by the Presidential Grant of the Russian Federation no. MK-8221.2016.2.

REFERENCES

1. A. J. Minnich, M. S. Dresselhaus, Z. F. Ren, and G. Chen, Energy Environ. Sci. **2**, 466 (2009).
2. L. D. Ivanova and A. A. Baikov, J. Thermoelectr. **3**, 60 (2009).
3. E. S. Demidov, E. D. Pavlova, and A. I. Bobrov, JETP Lett. **96**, 706 (2012).
4. E. S. Demidov, V. V. Podol'skii, V. P. Lesnikov, E. D. Pavlova, A. I. Bobrov, V. V. Karzanov, N. V. Malekhonova, and A. A. Tronova, JETP Lett. **100**, 719 (2014).
5. C. Gayner and K. K. Kar, Prog. Mater. Sci. **83**, 330 (2016).
6. I. V. Erofeeva, M. V. Dorokhin, V. P. Lesnikov, A. V. Zdoroveishchev, A. V. Kudrin, D. A. Pavlov, and Yu. V. Usov, Semiconductors **50**, 1453 (2016).
7. A. T. Burkov, A. I. Fedotov, A. A. Kas'yanov, R. I. Panteleev, and T. Nakama, Nauch.-Tekh. Vestn. Inf. Tekhnol., Mekh. Opt. **15**, 173 (2015).
8. D. G. Cahill, H. E. Fischer, T. Klitsner, E. T. Swartz, and R. O. Pohl, J. Vac. Sci. Techol. A **7**, 1259 (1989).
9. K. Maize, Y. Ezzahri, X. Wang, S. Singer, A. Majumdar, and A. Shakouri, in *Proceedings of the 24th Annual IEEE Semiconductor Thermal Measurement and Management Symposium, San Jose, CA, March 16–20, 2008*, p. 185.
10. D. G. Cahill, Rev. Sci. Instrum. **61**, 802 (1990).
11. S.-M. Lee, and D. G. Cahill, J. Appl. Phys. **81**, 2590 (1997).
12. T. Borca-Tasciuc, D. W. Song, J. R. Meyer, I. Vurgaftman, M.-J. Yang, B. Z. Nosho, L. J. Whitman, H. Lee, R. U. Martinelli, G. W. Turner, M. J. Manfra, and G. Chen, J. Appl. Phys. **92**, 4994 (2002).
13. C.-K. Liu, C.-K. Yu, H.-C. Chien, S.-L. Kuo, C.-Y. Hsu, M.-J. Dai, G.-L. Luo, S.-C. Huang, and M.-J. Huan, J. Appl. Phys. **104**, 114301 (2008).
14. *CRC Handbook of Thermoelectrics*, Ed. by D. M. Rowe (CRC, New York, 1995).
15. M. I. Fedorov, J. Thermoelectr. **2**, 51 (2009).

Translated by N. Korovin